FORMATION OF CORONAL LARGE-AMPLITUDE WAVES

Tomislav Žic[1] • Bojan Vršnak[1] • Slaven Lulić[2]

[1]Hvar Observatory, Faculty of Geodesy, Kačićeva 26, HR10000 Zagreb, Croatia

[2]Karlovac University of Applied Sciences, Trg J.J. Strossmayera 9, HR47000 Karlovac, Croatia

Introduction

An in-depth analysis of numerical simulations is performed to obtain a deeper insight into the nature of various phenomena occurring in the solar atmosphere as a consequence of the eruption of unstable coronal structures. Simulations take into account only the most basic characteristics of a flux-rope eruption and reveals important information on various eruption-related effects. It is shown that the eruption can cause an observable Moreton wave and a secondary coronal front only if it is powerful enough and is preferably characterized by significant lateral expansion.

The Model

The simulations were performed employing the Versatile Advection Code (VAC; Tóth, 1996; Goedbloed, Keppens, and Poedts, 2003) and setting:

- 2.5D model: $B_z(x,y) \neq 0$, $v_z = 0$, $\beta = 0$
- vertical profile of the density: solar atmosphere
- flux-rope magnetic field is defined as:

$$B_z(r) = \sqrt{B_{z0}^2 - \left(B_{z0}^2 - B_{ze}^2\right)\ \left(r/r_e\right)^2}$$

$$B_\phi(r) = \frac{B_{\phi e}}{2}\left[\sin\left(\frac{\pi r}{r_e} - \frac{\pi}{2}\right) + 1\right]$$

- B_{z0} represents the initial magnetic field at the center of the flux rope located at $x = 0$, $y = y_0$
- $B_{\varphi e}$ represents the initial poloidal field at the flux-rope boundary

Outside the flux-rope ($r > r_e$) :

- $B_{ze} = 0$,
- poloidal field is the potential field: $B_\varphi = B_{\varphi e}\, r_e/r$.

The runs are performed for the values of:

- the central field: B_{z0} = 5, 6, 7, 8, 9, 20, 50
- the initial height: y_0 = 0.20, 0.25, 0.30,
- the initial upward speed: v_{y0} = 1, 2, 3, 4, 5.

Results

The modelling reveals a rich variety of eruption-driven phenomena, reproducing nicely the typically observed eruption-associated signatures:

- a fast-mode MHD shock that propagates in all directions ahead of the expanding source-region.
- the source region expansion is subsonic in the helmet streamer configuration
- the shock formation is caused by a nonlinear evolution of the large-amplitude perturbation front driven by a subsonically expanding piston.

The max. Alfvén Mach number (M_A) of the source region is reached within $t \approx 0.02$:

- for $B_{z0} = 20$: $M_A \approx 0.5$,
  - shock forms at $x(t = 0.03) = 0.25$
- for $B_{z0} = 10$: $M_A \approx 0.1$
  - shock forms at $x(t = 0.07) = 0.35$

Comparison to the real situation:

- the background coronal Alfvén speed: v_{A0} = 300 km/s
- the numerical box a size of: λ = 450 Mm
- corresponding to the Alfvén travel time: $\tau_A = \lambda/v_{A0}$ = 1500 s

shows that the corresponding shock formation times ($\tau = t \times \tau_A$) and distances ($d = x \times \lambda$) are:

- τ = 45 s; d = 112 Mm
- τ = 105 s; d = 158 Mm

These numbers are consistent with the appearance of the coronal EUV waves, Moreton waves and the radio type II bursts.

After a phase of expanding source region:

- the coronal wave propagates as a large-amplitude "simple wave" by:

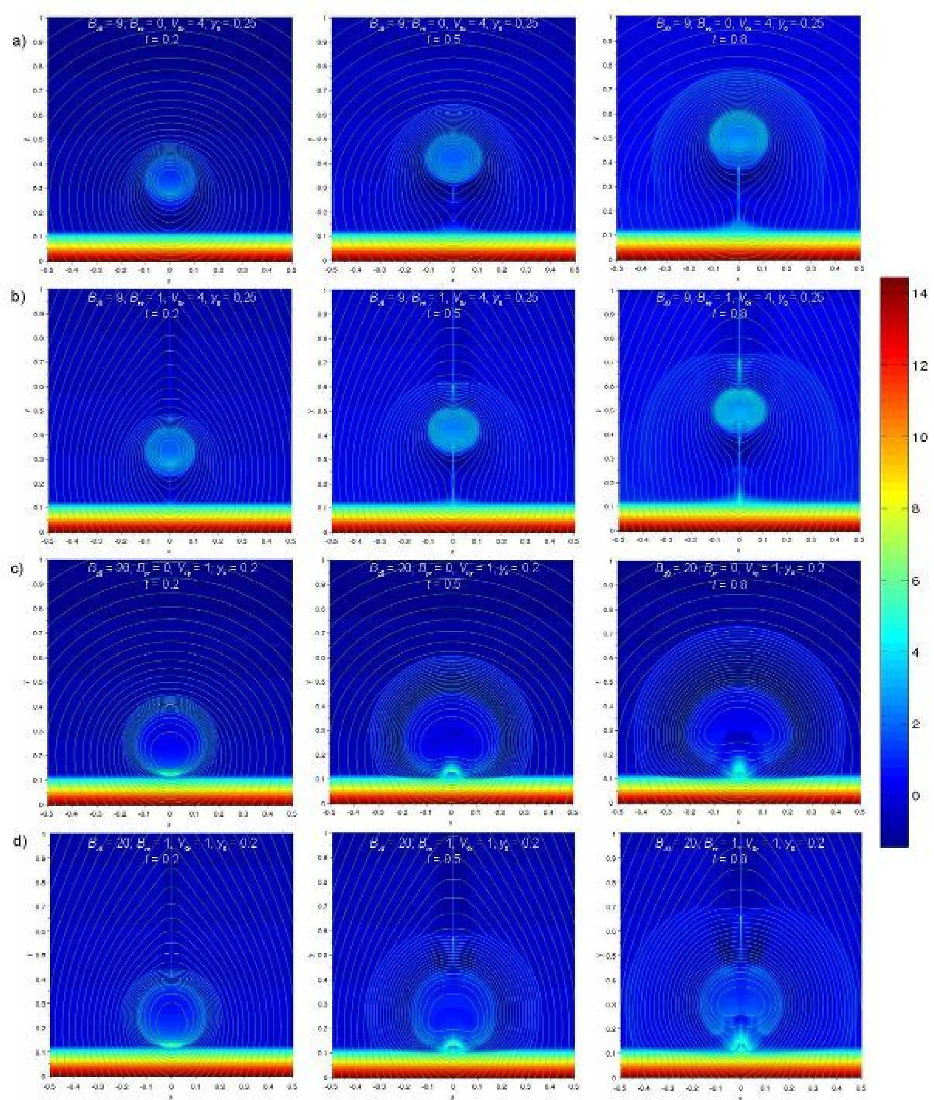

Fig. 1. Evolution of the coronal disturbance driven by different types of the eruption: a) and b) eruption dominated by vertical motion (weak flux-rope expansion); c) and d) eruption dominated by overexpansion. Two background coronal magnetic field configurations are considered: a) and c) purely potential arcade field ($B_{ye} = 0$); b) and d) helmet streamer configuration ($B_{ye} = 1$). The left, middle, and right columns show snapshots taken at t = 0.02, 0.05, and 0.08. White lines represent the magnetic field lines; the density is color-coded (logarithmic scale; $\rho = e^\alpha$, where α is written in the displayed color-code scale. Input parameters are written at the top of each panel.

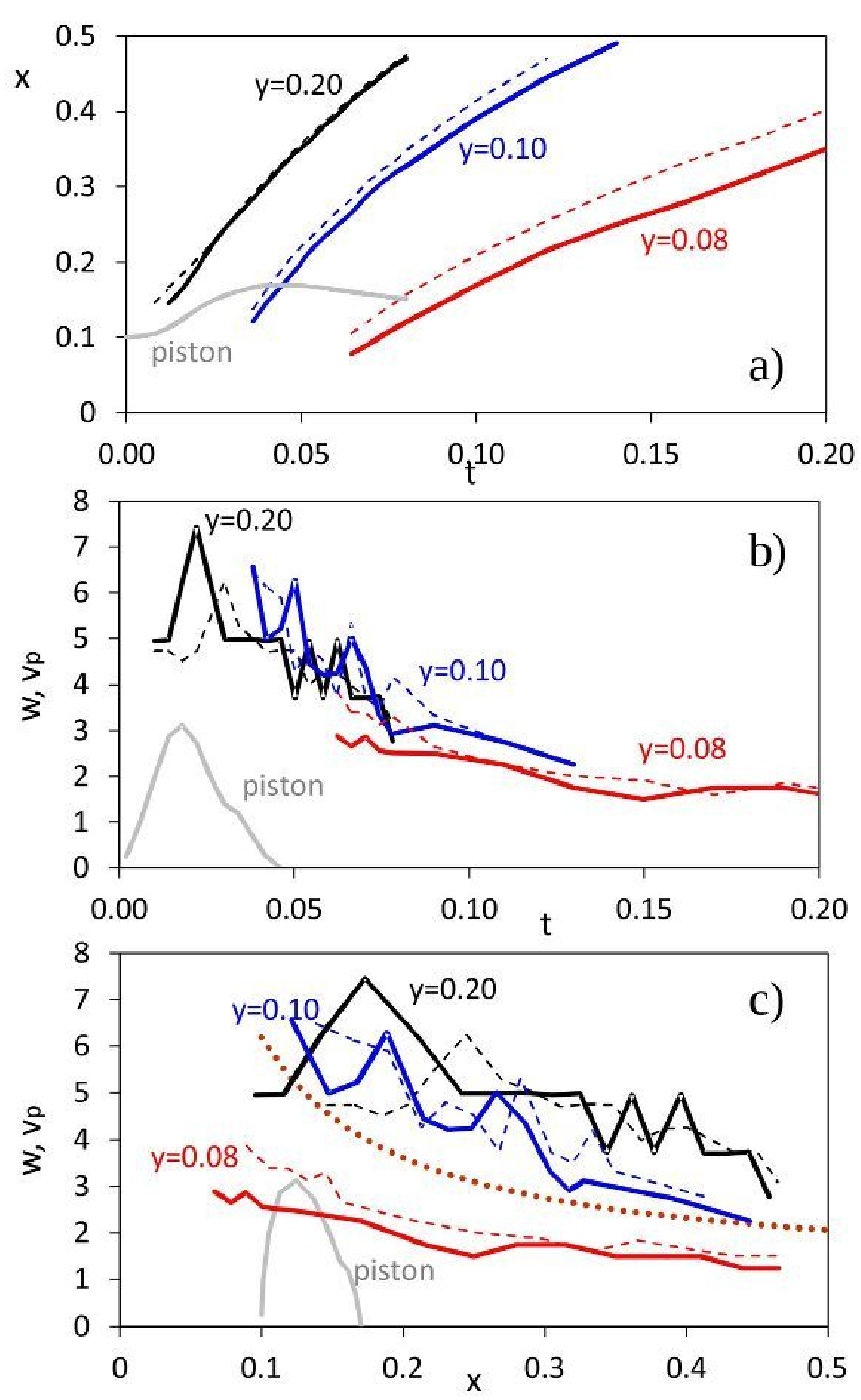

Fig. 2. The x-direction kinematics of the wavefront in the helmet streamer configuration ($B_{ye} = 1$), measured at three different heights for $B_{z0} = 20$. The y-coordinate is written by the curves. Gray line represents the motion of the contact surface (denoted as "piston") at the height of $y = 0.2$, *i.e.*, at the initial height of the flux-rope center. Panel a) show the distance–time curves $x(t)$ of the wavefront leading edge (dashed lines) and the wave crest (solid lines). Panel b) display the corresponding phase speeds $w(t)$ and the piston velocity $v_p(t)$. In panel c) these velocities are shown as a function of distance $w(x)$, $v_p(x)$; the brown dotted line shows the ambient Alfvén speed at the height $y = 0.2$.

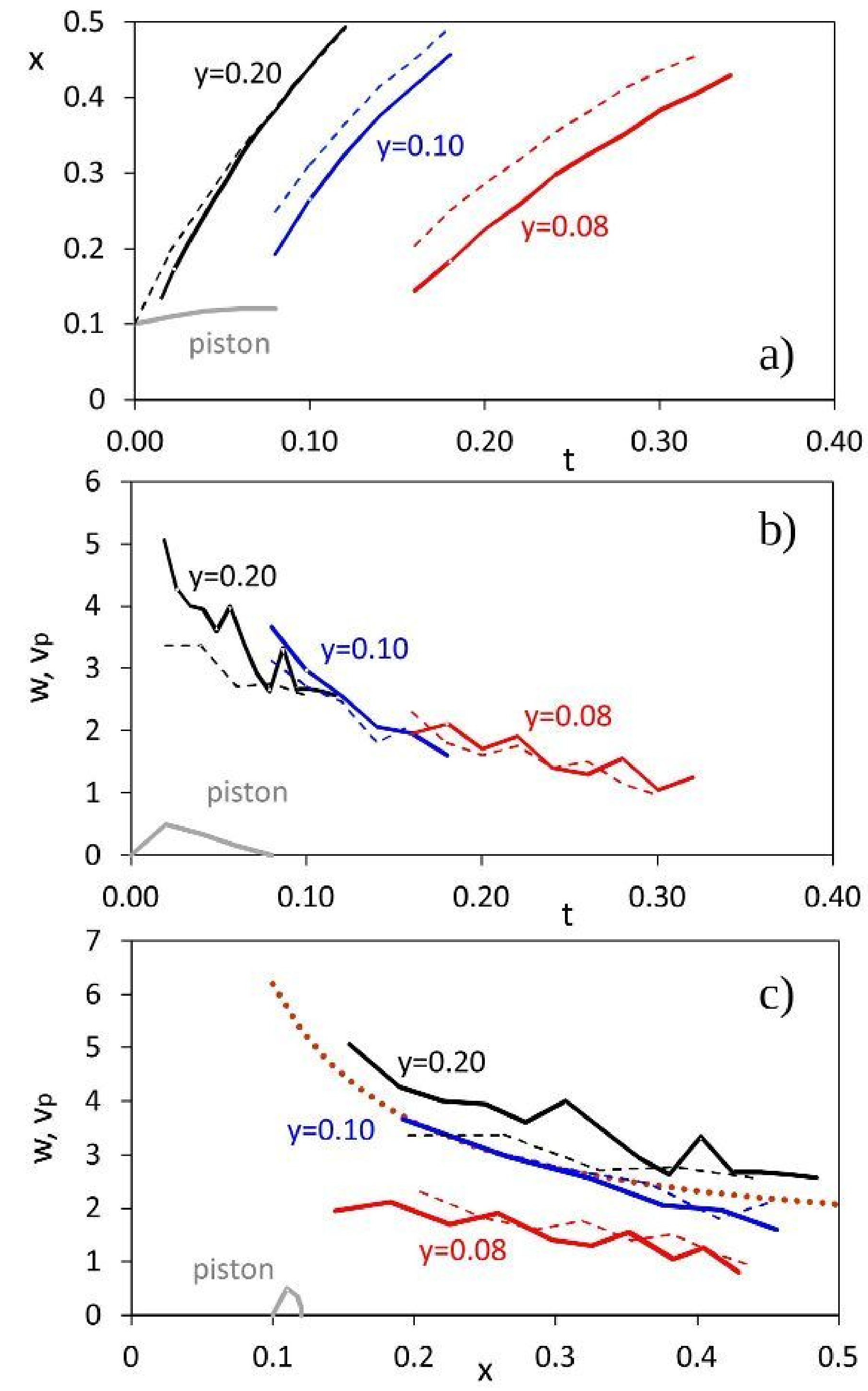

Fig. 3. The x-direction kinematics of the wavefront in the helmet streamer configuration ($B_{ye} = 1$), measured at three different heights for $B_{z0} = 10$. The y-coordinate is written by the curves. Gray line represents the motion of the contact surface (denoted as "piston") at the height of $y = 0.2$, *i.e.*, at the initial height of the flux-rope center. Panel a) show the distance–time curves $x(t)$ of the wavefront leading edge (dashed lines) and the wave crest (solid lines). Panel b) display the corresponding phase speeds $w(t)$ and the piston velocity $v_p(t)$. In panel c) these velocities are shown as a function of distance $w(x)$, $v_p(x)$; the brown dotted line shows the ambient Alfvén speed at the height $y = 0.2$.

- the increasing size of the expanding wave-front,
- the evolution of the wave amplitude,
- the change of the background Alfvén speed along the direction of propagation.

The coronal shock passage:

- impulsively exerts a downward compression on the transition region and chromosphere
- perturbation propagates downward as a quasi-longitudinal MHD shock
- the strong disturbance is able to create an observable Moreton wave

Conclusion

It is shown that even a relatively simple 2.5D numerical simulation provides an in-depth insight into the nature of various phenomena occurring as a consequence of the eruption. It directly relates properties of the eruption with the characteristics and evolution of the expanding large-amplitude coronal fast-mode MHD wave (observed as fast EUV coronal waves and radio type II bursts) and the related chromospheric downward-propagating quasi-longitudinal perturbation (resulting in a Moreton wave). Moreover, it reveals the nature of secondary effects such as coronal upflows, secondary shocks, various forms of wave-trains, delayed large-amplitude slow disturbances, transient coronal dimmings, and chromospheric relaxation.

Acknowledgments

We acknowledge the support of European Social Fund under the „PoKRet" project.